Appl. Math. Mech. -Engl. Ed., **32**(8), 997–1008 (2011)
DOI 10.1007/s10483-011-1475-6

Applied Mathematics and Mechanics (English Edition)

Application and analysis of functionally graded piezoelectrical rotating cylinder as mechanical sensor subjected to pressure and thermal loads*

G. H. RAHIMI, M. AREFI, M. J. KHOSHGOFTAR

(Department of Mechanical Engineering, Tarbiat Modares University, Tehran 14115-143, Iran)

Abstract The exact thermoelastic analysis of a functionally graded piezoelectrical (FGP) rotating cylinder is investigated analytically. The cylinder is subjected to a combination of electrical, thermal, and mechanical loads simultaneously. The structure is a simplified model of a rotational sensor or actuator. The basic governing differential equation of the system is obtained by using the energy method. A novel term, named as the additional energy, is introduced to exact the evaluation of the energy functional. The solution to the governing differential equation is presented for two types of boundary conditions including free rotating and rotating cylinders exposed to the inner pressure. The effect of the angular velocity is investigated on the radial distribution of various components. The mentioned structure can be considered as a sensor for measuring the angular velocity of the cylinder subjected to the pressure and temperature. The obtained results indicate that the electrical potential is proportional to the angular velocity.

Key words functionally graded piezoelectric (FGP) material, sensor, rotating cylinder, angular velocity, pressure, temperature

Chinese Library Classification O343.6
2010 Mathematics Subject Classification 74F05

Nomenclature

C,	elastic stiffness;	u,	displacement;
D,	electrical displacement;	$W_{\rm b}$,	body force energy;
e,	piezoelectric coefficient;	$Q_{\rm T}$,	additional energy;
k,	heat conductivity coefficient;	J,	Jacobin;
p,	pyroelectric coefficient;	α,	heat expansion coefficient;
$P_{\rm i}$,	inner pressure;	φ,	electrical potential;
r,	radius;	η,	dielectric coefficient;
E_r,	electrical field;	σ,	stress;
T,	temperature;	ε,	strain.

1 Introduction

Piezoelectric material can be used in electromechanical systems, such as sensors and actuators. It has the ability to produce electricity when it subjected to mechanical stress. The application of functionally graded piezoelectric materials (FGPMs) can control the distribution of the mechanical and electrical components with appropriate precision.

* Received Oct. 27, 2010 / Revised May 9, 2011
Corresponding author G. H. RAHIMI, Associate Professor, Ph. D., E-mail: rahimi_gh@modares.ac.ir

The effects of the rotational load on the mechanical and electrical components for an inhomogenous structure and application of the energy method have been widely studied with the thermoelastic analysis of an inhomogenous structure. Liu et al.[1] presented an analytical model for free vibration analysis of the piezoelectric coupled moderately thick circular plate based on Mindlin's plate theory, and extracted four differential equations for four unknown components, i.e., the displacement, two rotations, and the electrical potential field. Hou and Leung[2] investigated the dynamic analysis of a magneto-piezoelectric hollow cylinder, and offered a simple and accurate tool for the prediction, identification, and study of the complex dynamic characteristics of coupling mechanical and electromagnetic fields. Kollias and Avaritsiotis[3] proposed the method of eigenfunction expansion for an analytical expression for the frequency response of a bending mode piezoelectric accelerometer system, and showed that the used approximate relation were validated with experimental responses. Dai and Wang[4] presented an analytical solution for the stress wave propagation in piezoelectric fiber reinforced laminated composites subjected to thermal shock loading by means of finite Hankel transforms and Laplace transforms. Pietrzakowski[5] investigated the vibration analysis of active rectangular plates. Babaei and Chen[6] presented the exact solution of an infinitely long magnetoelastic hollow cylinder and a solid rotating cylinder polarized and magnetized radially. Khoshgoftar et al.[7] investigated the thermoelastic analysis of a thick walled cylinder made of the FGPM. They supposed that all mechanical and electrical properties varied functionally. However, there is no experimental report for various structures on the production and manufacturing of the FGPMs. Therefore, the theoretical method may be evaluated as a novel method for the analysis.

The present paper aims to investigate the application and analysis of a functionally graded piezoelectric (FGP) cylinder as a sensor or an actuator in electromechanical systems. The thermoelastics is analyzed by using the energy method. A novel term, defined as the additional energy, is proposed for the prediction of the behaviors of piezoelectric structures, especially exposed to thermal loads. An FGP hollow cylinder fixed on the rotary devices is introduced to measure the angular velocity. The results show that the present study can be used to predict the behavior of an FGP rotating cylinder subjected to various angular velocities.

2 Solution to heat conduction equation

In this section, the symmetric and steady-state heat transfer equation in the cylindrical coordinate system is solved with the assumed boundary conditions. The symmetric and steady-state heat transfer equation in the cylindrical coordinate system can be represented as follows[8–9]:

$$\frac{1}{r}(rk_{\mathrm{T}}(r)T'(r))' = 0, \quad a \leqslant r \leqslant b, \tag{1}$$

where a and b are the inner and outer radii, respectively. $k_{\mathrm{T}}(r)$ is the thermal conductivity which is assumed to be a function of the radius r. General boundary conditions for Eq. (1) are[8,10]

$$\begin{cases} C_{11}T(a) + C_{12}T'(a) = f_1, \\ C_{21}T(b) + C_{22}T'(b) = f_2, \end{cases} \tag{2}$$

where C_{ij} $(i, j = 1, 2)$ are the constants depending on the thermal conductivity and the thermal convection. f_1 and f_2 are the constants evaluated at the inner and outer radii, respectively.

Based on the inhomogenous distribution of the material properties, the heat conduction coefficient can be assumed as follows:

$$k_{\mathrm{T}}(r) = k_0 r^k, \tag{3}$$

where k is an inhomogenous index. The general solution to the temperature distribution can be obtained by

$$T(r) = \frac{-A_1}{k} r^{-k} + A_2, \quad k \neq 0, \tag{4}$$

where A_1 and A_2 are the constants of the integration given by

$$\begin{cases} A_1 = \dfrac{C_{21} f_1 - C_{11} f_2}{C_{21}\big(C_{12} r_a^{-(k+1)} - C_{11} \frac{r_a^{-k}}{k}\big) - C_{11}\big(C_{22} r_b^{-(k+1)} - C_{21} \frac{r_b^{-k}}{k}\big)}, \\ A_2 = \dfrac{\big(C_{12} r_a^{-(k+1)} - C_{11} \frac{r_a^{-k}}{k}\big) f_2 - f_1\big(C_{22} r_b^{-(k+1)} - C_{21} \frac{r_b^{-k}}{k}\big)}{C_{21}\big(C_{12} r_a^{-(k+1)} - C_{11} \frac{r_a^{-k}}{k}\big) - C_{11}\big(C_{22} r_b^{-(k+1)} - C_{21} \frac{r_b^{-k}}{k}\big)}. \end{cases} \tag{5}$$

3 Piezothermoelastic analysis

In this section, the necessary equations for an FGP rotating cylinder are derived. Due to the symmetric boundary conditions and the applied loads, the strain-displacement relations for only one nonzero displacement component (radial displacement) are as follows[11–12]:

$$\varepsilon_{rr} = \frac{\partial u}{\partial r}, \quad \varepsilon_{\theta\theta} = \frac{u}{r}, \quad u = u(r). \tag{6}$$

The schematic figure of an FGP rotating cylinder is shown in Fig. 1. The cylinder is assumed to be uniform in the axial direction. The present condition is actually the model of an infinite cylinder valid for many applied problems.

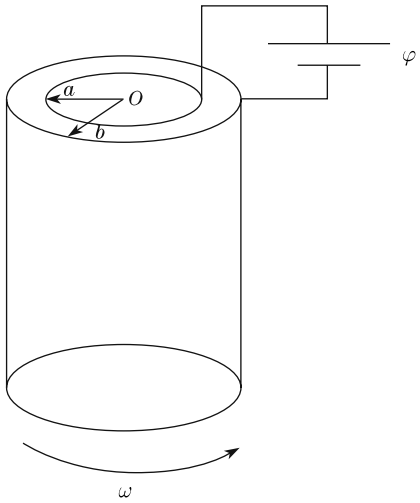

Fig. 1 Schematic figure of FGP rotating cylinder

For an electromechanical structure, due to the exposed electrical potential on the boundaries of the structure, an electrical field can be expected as follows[6–7]:

$$\begin{cases} \varphi = \varphi(r), \quad E = -\nabla\varphi, \\ E_r = -\dfrac{\partial \varphi}{\partial r}, \quad E_\theta = E_z = 0. \end{cases} \tag{7}$$

Considering the coupled equations between the mechanical, thermal, and electrical components, two nonzero components of the stress are[7]

$$\begin{cases} \sigma_{rr} = C_{rr}\varepsilon_{rr} + C_{r\theta}\varepsilon_{\theta\theta} - e_{rr}E_r - \beta_r T, \\ \sigma_{\theta\theta} = C_{r\theta}\varepsilon_{rr} + C_{\theta\theta}\varepsilon_{\theta\theta} - e_{r\theta}E_r - \beta_\theta T, \end{cases} \tag{8}$$

where $\sigma_{r\theta}$ is zero due to the symmetry. σ_{ij} and ε_{ij} $(i,j = r,\theta)$ are the components of the stress and strain tensors. $T(r)$ is the temperature distribution. $E(r)$ is the electrical field. C_{ij} $(i,j = r,\theta)$ are the elastic stiffness, and e_{ij} $(i,j = r,\theta)$ are the piezoelectric coefficients. β can be obtained from[7]

$$\begin{cases} \beta_r = C_{rr}\alpha_r + C_{r\theta}\alpha_\theta, \\ \beta_\theta = C_{r\theta}\alpha_r + C_{\theta\theta}\alpha_\theta, \end{cases} \tag{9}$$

where α_i $(i = r,\theta)$ are the coefficients of the thermal expansion.

The electrical displacement, including the strain, electrical field, and temperature, can be written as follows[7]:

$$D_r = e_{rr}\varepsilon_{rr} + e_{r\theta}\varepsilon_{\theta\theta} + \eta E_r - pT, \tag{10}$$

where η is the dielectric constant, and p is the pyroelectric constant. Due to the symmetric condition, the circumferential component of the electrical displacement D_θ is zero.

Before substituting the component of the electrical field in the energy equation, the appropriate functions for all properties are assumed by using the power function to be[7]

$$\begin{cases} \rho = \rho_0 r^l \eta = \eta_0 r^l, \quad e_{ri} = e_{ri0} r^l, \quad C_{ij} = C_{ij0} r^l, \\ p = p_0 r^{b+l}, \quad \beta = \beta_0 r^{b+l}, \quad \alpha = \alpha_0 r^b, \end{cases} \tag{11}$$

where l and b are the inhomogenous parameters of the material properties. The energy per unit volume of a rotating cylinder is

$$\overline{u} = \frac{1}{2}\left(\varepsilon^{\mathrm{T}}\sigma - D^{\mathrm{T}}E - Q_{\mathrm{T}}T\right) - W_{\mathrm{b}}, \tag{12}$$

where

$$Q_{\mathrm{T}} = \sum_{i=1}^{3} (\beta_i \varepsilon_{ii} - pE_i). \tag{13}$$

The appropriate functional $F(u,\varphi,r)$ for the assumed structure in the cylindrical coordinate system is

$$F(u,\varphi,r) = |J|\,\overline{u} = r\overline{u}, \tag{14}$$

where J is the Jacobin of each arbitrary coordinate system. For this problem, we have

$$\begin{aligned} F(u,\varphi,r) = \pi\Big(& r\Big(C_{rr0}r^l\frac{\partial u}{\partial r} + C_{r\theta0}r^l\frac{u}{r} + e_{rr0}r^l\frac{\partial\varphi}{\partial r} - \beta_{r0}r^{b+l}T\Big)\frac{\partial u}{\partial r} \\ & + r\Big(C_{r\theta0}r^l\frac{\partial u}{\partial r} + C_{\theta\theta0}r^l\frac{u}{r} + e_{r\theta0}r^l\frac{\partial\varphi}{\partial r} - \beta_{r0}r^{b+l}T\Big)\frac{u}{r} \\ & + r\Big(e_{rr0}r^l\frac{\partial u}{\partial r} + e_{r\theta0}r^l\frac{u}{r} - \eta_0 r^l\frac{\partial\varphi}{\partial r} - p_0 r^{b+l}T\Big)\frac{\partial\varphi}{\partial r}\Big) \\ & - r\Big(\beta_{r0}r^{b+l}\frac{\partial u}{\partial r} + \beta_{\theta0}r^{b+l}\frac{u}{r} + p_0 r^{b+l}\frac{\partial\varphi}{\partial r}\Big)T \\ & - 2\pi\rho_0 r^l r^2\omega^2 u. \end{aligned} \tag{15}$$

Imposing the Euler equations

$$\frac{\partial F}{\partial q_i} - \frac{\partial}{\partial r}\frac{\partial F}{\partial(\frac{\partial q_i}{\partial r})} = 0, \quad q_i = u, \varphi$$

to the above functional, the system of the differential equation can be obtained as follows:

$$\begin{cases} (C_{rr0})r^2\dfrac{\partial^2 u}{\partial r^2} + (C_{rr0}(l+1))r\dfrac{\partial u}{\partial r} + (C_{r\theta 0}l - C_{\theta\theta 0})u \\ \quad + (e_{rr0})r^2\dfrac{\partial^2 \varphi}{\partial r^2} + (e_{rr0}(l+1) - e_{r\theta 0})r\dfrac{\partial \varphi}{\partial r} \\ = -A_1\Big(\beta_{r0}\Big(1 - \dfrac{1}{k}(b+l+1)\Big) + \dfrac{1}{k}\beta_{\theta 0}\Big)r^{b-k+1} \\ \quad - A_2(-\beta_{r0}(b+l+1) + \beta_{\theta 0})r^{b+1} - \rho_0 r^3\omega^2, \\ (e_{rr0})r^2\dfrac{\partial^2 u}{\partial r^2} + (e_{rr0}(l+1) + e_{r\theta 0})r\dfrac{\partial u}{\partial r} + (e_{r\theta 0}l)u \\ \quad - (\eta_0)r^2\dfrac{\partial^2 \varphi}{\partial r^2} - (\eta_0(l+1))r\dfrac{\partial \varphi}{\partial r} \\ = -p_0 A_1\Big(\dfrac{1}{k}(b+l+1) - 1\Big)r^{b-k+1} + p_0 A_2(b+l+1)r^{b+1}. \end{cases} \tag{16}$$

It indicates that when $\omega = 0$, Eq. (16) is exactly the same as Eqs. (15-a) and (15-b) in Ref. [7].

The solutions to Eq. (16) include homogenous and particular solutions. The homogenous solution to Eq. (16) can be obtained with composing the characteristic equation of the governing differential equation and evaluating the roots. Primarily, it is appropriate to convert the Cauchy-Euler equation (see Eq. (16)) into a solvable differential equation with the transformation $r = \mathrm{e}^s$. With the definition of $\lambda = \frac{\mathrm{d}}{\mathrm{d}s}$, the homogenized differential equation can be expressed as follows:

$$\begin{cases} (C_{rr0}\lambda^2 + C_{rr0}l\lambda + C_{r\theta 0}l - C_{\theta\theta 0})u + (e_{rr0}\lambda^2 + (e_{rr0}l - e_{r\theta 0})\lambda)\varphi = 0, \\ (e_{rr0}\lambda^2 + (e_{rr0}l + e_{r\theta 0})\lambda + le_{r\theta 0})u + (-\eta_0\lambda^2 - \eta_0 l\lambda)\varphi = 0. \end{cases} \tag{17}$$

The nontrivial solution to Eq. (17) can be obtained with evaluating the determinant of this equation and evaluating the roots by

$$\lambda^4 + 2l\lambda^3 + (l^2 + \gamma)\lambda^2 + l\gamma\lambda = 0. \tag{18}$$

After evaluating the roots, the homogenous solution to the problem (u_{h} and φ_{h}) can be obtained by using the following method:

$$\begin{cases} u_{\mathrm{h}} = \displaystyle\sum_{i=1}^{4} u_{\mathrm{h}i}r^{\lambda_i}, \quad \varphi_{\mathrm{h}} = \sum_{i=1}^{4} M_i u_{\mathrm{h}i}r^{\lambda_i}, \\ M_i = -\dfrac{C_{rr0}\lambda_i^2 + C_{rr0}l\lambda_i + C_{r\theta 0}l - C_{\theta\theta 0}}{e_{rr0}\lambda_i^2 + (e_{rr0}l - e_{r\theta 0})\lambda_i}, \end{cases} \tag{19}$$

where $u_{\mathrm{h}i}$ $(i = 1, 2, 3, 4)$ are the constants of the problem which can be obtained by imposing the four mechanical and electrical boundary conditions.

The fourth-order characteristic equation can be solved to evaluate the roots of the characteristic equation. The values of the roots can define the homogenous solution directly.

The particular solution to the system depends on the right-hand of the differential equation of the system. At the right-hand side of Eq. (16), three types of terms exist, i.e., r^{b-k+1}, r^{b+1}, and r^3. Considering the mentioned sentences, the particular solutions to Eq. (16) are

$$\begin{cases} u_{\mathrm{p}} = X_1 r^{b-k+1} + X_2 r^{b+1} + X_3 r^3, \\ \varphi_{\mathrm{p}} = X_4 r^{b-k+1} + X_5 r^{b+1} + X_6 r^3, \end{cases} \tag{20}$$

where X_i $(i = 1, 2, \cdots, 6)$ are unknown coefficients. These coefficients can be obtained by substituting Eq. (20) into Eq. (16) and equaling the same terms at two sides of the differential equations. Therefore, the solution to the system of the differential equation is

$$u = u_{\mathrm{h}} + u_{\mathrm{p}}, \quad \varphi = \varphi_{\mathrm{h}} + \varphi_{\mathrm{p}}. \tag{21}$$

The final solution includes four constants of integration $u_{\mathrm{h}i}$ $(i = 1, 2, 3, 4)$. These constants may be obtained with imposing the appropriate mechanical and electrical boundary conditions.

4 Numerical results for two types of boundary conditions

4.1 Rotating cylinder with free-free boundary condition

The final solution can be obtained by devoting the numerical values to the parameters and applying the boundary conditions to the problem. The numerical parameters for the presentation of the results can be considered as follows:

$$\begin{cases} \alpha_{r0} = 2.458 \times 10^{-6}\ \mathrm{K}^{-1}, \quad \alpha_{\theta 0} = 4.396 \times 10^{-6}\ \mathrm{K}^{-1}, \quad C_{rr0} = 83.6\ \mathrm{GPa}, \\ C_{\theta\theta 0} = 74.1\ \mathrm{GPa}, \quad C_{r\theta 0} = 39.3\ \mathrm{GPa}, \quad e_{rr0} = 0.347\ \mathrm{C \cdot m^{-2}}, \quad e_{r\theta 0} = 0.16\ \mathrm{C \cdot m^{-2}}, \\ \eta_0 = 9.03 \times 10^{-11}\ \mathrm{C^2 \cdot N^{-1} \cdot m^{-2}}, \quad p_0 = 2.94 \times 10^{-6}\ \mathrm{C \cdot m^{-2} \cdot K^{-1}}. \end{cases} \tag{22}$$

In our analyses, the thermal loading is considered as a permanent loading. Therefore, the present model can be considered as a mechanical sensor for measuring the angular velocity subjected to the thermal loading. The inner and outer temperatures are considered to be 50°C and 0°C, respectively.

There are two mechanical boundary conditions and two electrical boundary conditions in this problem. The mechanical boundary conditions for the free rotation of the cylinder are

$$u(r = a) = 0, \quad u(r = b) = 0. \tag{23}$$

The electrical boundary conditions for this type of boundary conditions of the cylinder are

$$\varphi(r = a) = 0, \quad \varphi(r = b) = 0. \tag{24}$$

The nondimensional parameters and angular velocity can be, respectively, selected by the following equations:

$$\begin{cases} \bar{\sigma} = \dfrac{\sigma}{\alpha_0 Y_0 T_0}, \quad \bar{\varepsilon} = \dfrac{\varepsilon}{\alpha_0 T_0}, \quad \bar{u}_r = \dfrac{u_r}{\alpha_0 T_0 r_b}, \quad \bar{e} = \dfrac{e}{Y_0 \left|d_0\right|}, \\ \bar{\eta} = \dfrac{\eta}{Y_0 \left|d_0\right|^2}, \quad \bar{p} = \dfrac{p}{\alpha_0 Y_0 \left|d_0\right|}, \quad \overline{D}_r = \dfrac{D_r}{\alpha_0 Y_0 T_0 \left|d_0\right|}, \quad \overline{\varphi} = \dfrac{\varphi \left|d_0\right|}{\alpha_0 T_0 r_b}, \\ \overline{E}_r = \dfrac{E_r \left|d_0\right|}{\alpha_0 T_0}, \quad \overline{T} = \dfrac{T}{T_0}, \quad \bar{r} = \dfrac{r}{r_b}, \quad \bar{\alpha} = \dfrac{\alpha}{\alpha_0}, \quad \overline{C}_{ij} = \dfrac{C_{ij}}{Y_0}, \end{cases} \tag{25}$$

$$\Omega = \frac{\omega}{\omega_0} \rightarrow \omega_0 = \frac{\alpha_0 Y_0 T}{\rho_0 r_b^2}, \tag{26}$$

In Eq. (11), three inhomogenous indexes are selected, i.e., l, b, and k. To evaluate the effect of the inhomogenous index, only l is selected to be a variable[7], the other variables are selected to be constants, i.e., $b = 0$ and $k = 0.01$. For evaluating the effect of the angular velocity on the mechanical and electrical components, four figures for each mechanical and electrical component are considered, which devote to four dimensionless angular velocities Ω, as shown in Figs. 2–4.

Figure 2 shows the distribution of the electrical potential along the thickness for four angular velocities. It indicates that the maximum value of the electrical potential is proportional to the dimensionless angular velocity Ω. The result can be applied to a mechanical sensor.

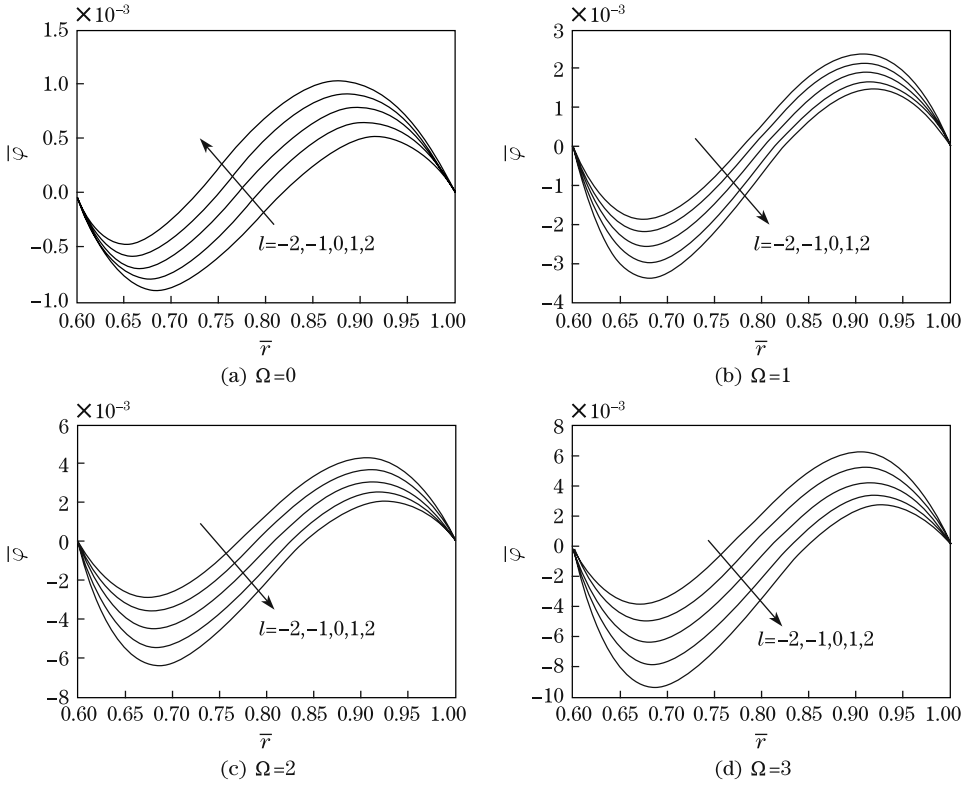

Fig. 2 Distribution of electrical potential with various Ω for five l under free rotation

Figure 3 shows the distribution of the radial displacement along the thickness for four angular velocities. It indicates that the value of the radial displacement is not proportional to Ω. The trend in Fig. 3 is the same for various Ω.

Figure 4 shows the distribution of the radial stress along the thickness for four angular velocities. It shows that the distributions have an intersection point for all inhomogenous indexes in which the radial stress is identical for all curves. This intersection point is an identical radial position for all angular velocities.

4.2 Rotating cylinder subjected to inner pressure

In this section, a pressurized rotating FGP cylinder subjected to the inner pressure is considered. The homogenous boundary condition is applied for the electrical potential. The mechanical boundary conditions for a rotating cylinder subjected to the inner pressure are

$$\sigma_{rr}(r = a) = -P_{\mathrm{i}}, \quad \sigma_{rr}(r = b) = 0, \tag{27}$$

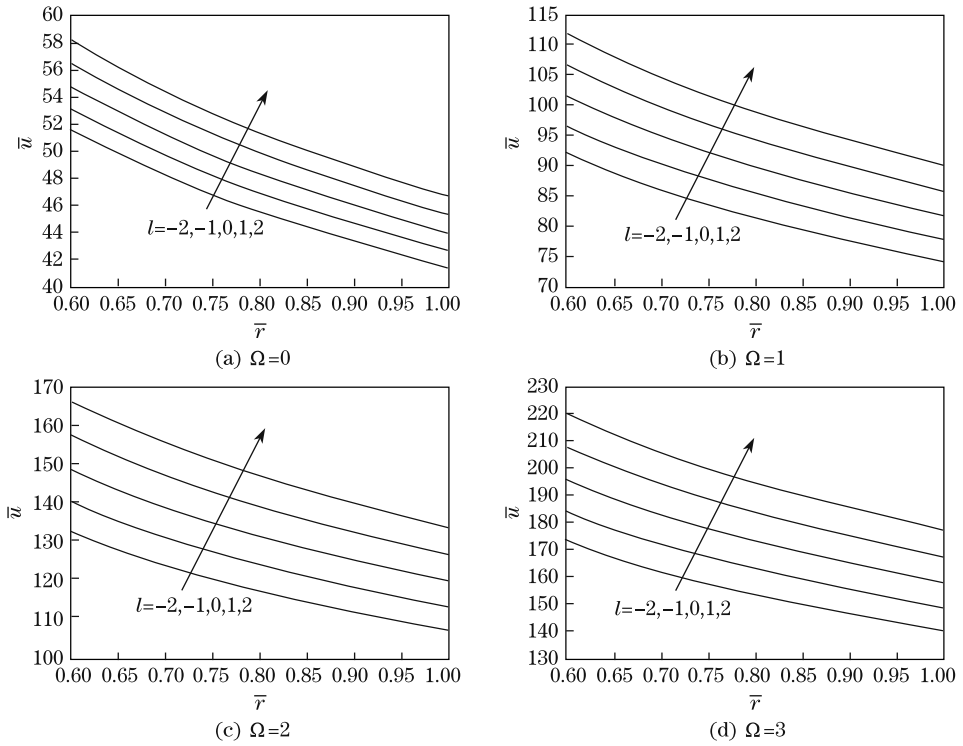

Fig. 3 Distribution of radial displacement with various Ω for five l under free rotation

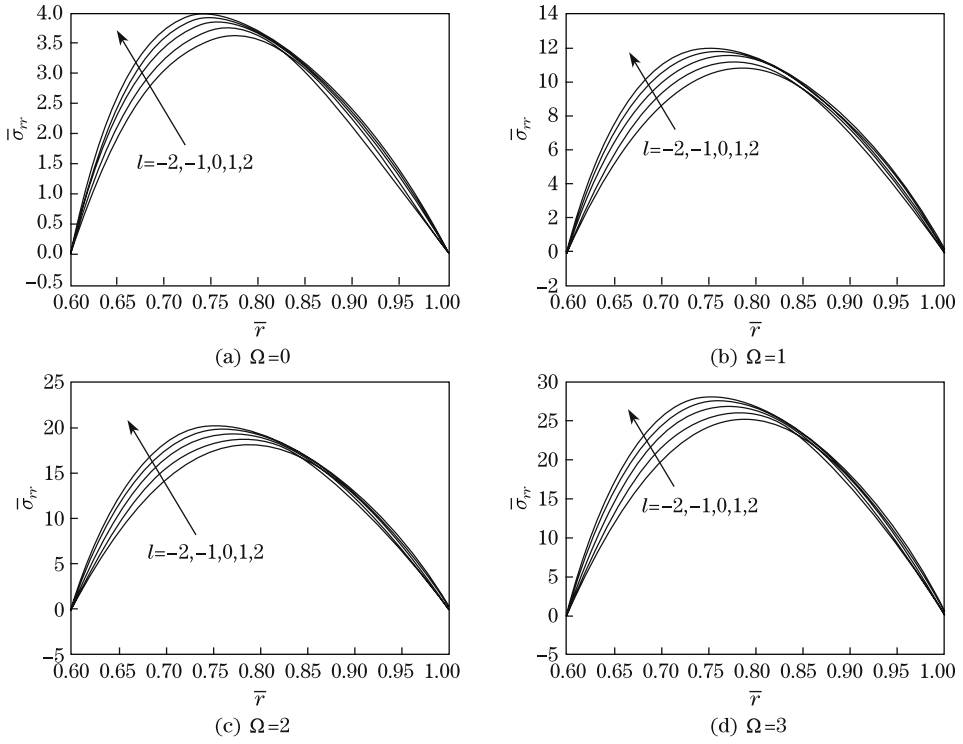

Fig. 4 Distribution of radial stress with various Ω for five l under free rotation

where P_{i} is the pressure at the inner radius of the cylinder. This boundary condition is the physical model of a hollow cylinder shrinking fit to a shaft. The homogenous electrical boundary conditions for the mentioned cylinder are

$$\varphi(r=a)=0, \quad \varphi(r=b)=0. \tag{28}$$

Imposing the appropriate boundary conditions, the distribution of the mechanical and electrical components can be evaluated analytically. For better understanding the effect of the angular velocity on the response of a pressurized FGP rotating cylinder, three electrical and mechanical components are selected, i.e., the radial stress, the radial displacement, and the electrical potential.

Figure 5 shows the distribution of the electrical potential along the thickness direction for four angular velocities. This figure indicates that the maximum value of the electrical potential is proportional to the dimensionless angular velocity Ω. This result has been obtained in the previous section for free rotation of the FGP cylinder.

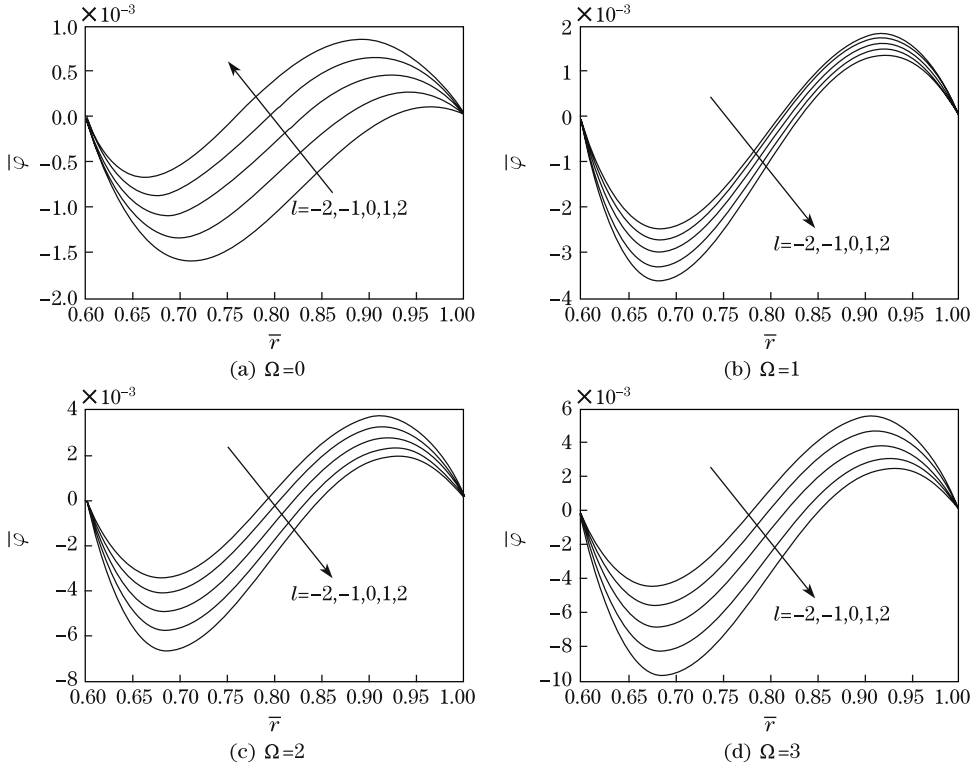

Fig. 5 Distribution of electrical potential with various Ω for five l under pressurized rotational cylinder

Figure 6 shows the distribution of the radial displacement along the thickness direction for four angular velocities. This figure indicates that the value of the radial displacement is not proportional to Ω. The trend in Fig. 6 is the same for different Ω. This result has been obtained in the previous section for the free rotation of the FGP cylinder.

Figure 7 shows the distribution of the radial stress along the thickness for four angular velocities. The same behavior shown in Fig. 4 can be understood for the free rotation of the FGP cylinder. An intersection point is located in an identical radial position for all angular velocities.

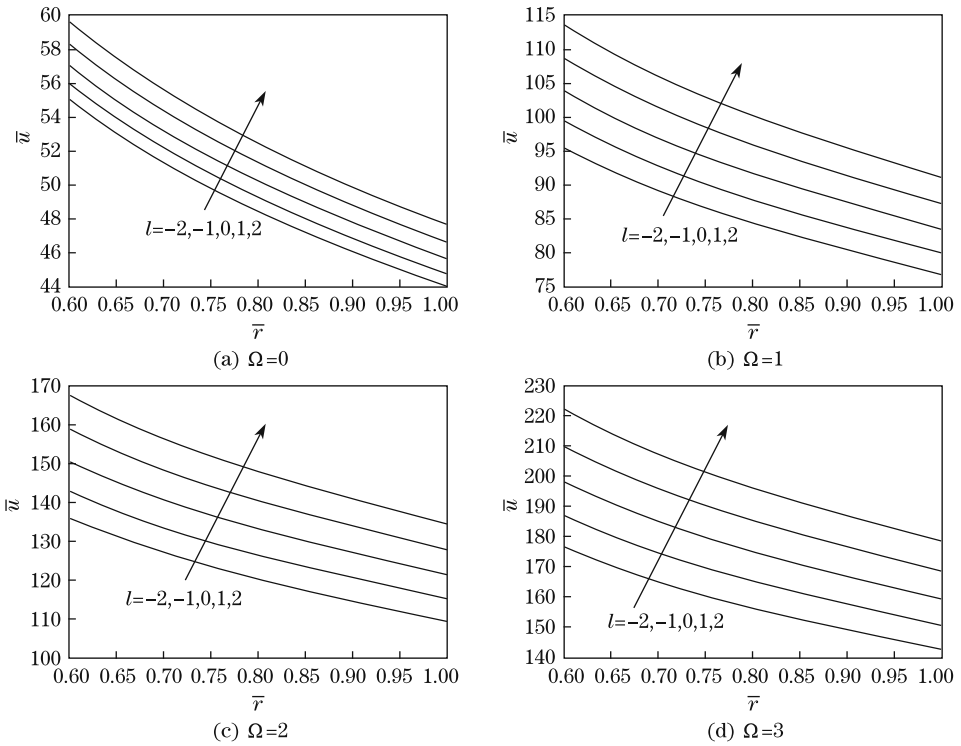

Fig. 6 Distribution of radial displacement with various Ω for five l under pressurized rotational cylinder

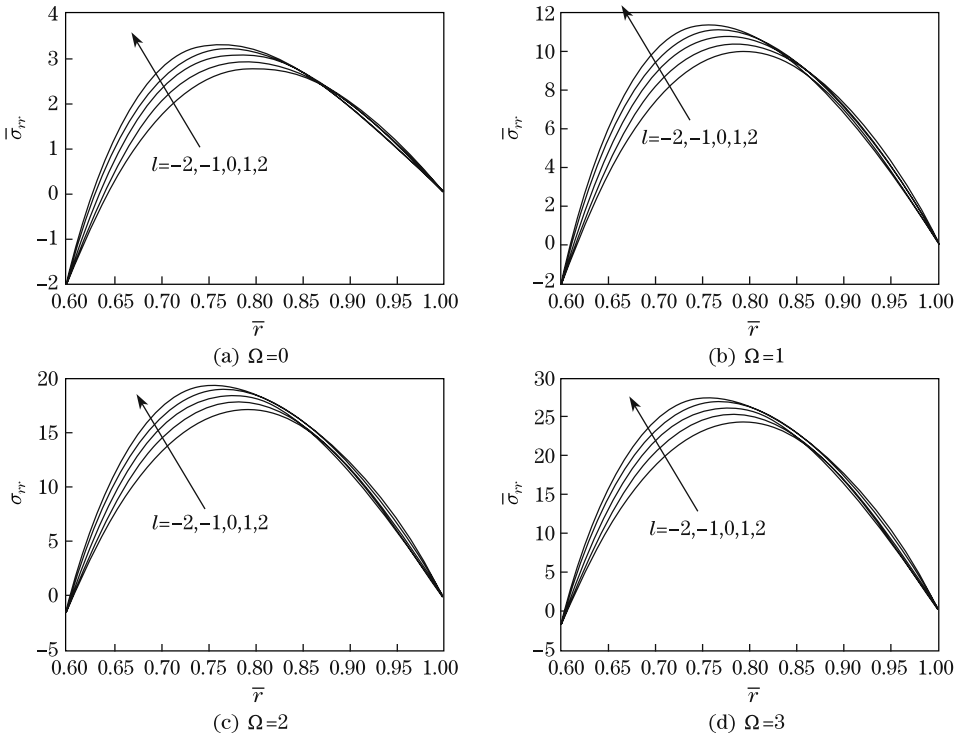

Fig. 7 Distribution of radial stress with various Ω for five l under pressurized rotational cylinder

4.3 Comparison between results of two types of studied cylinders

For better understanding the effect of an inner pressure on the response of an FGP rotating cylinder, the radial stress of an FGP rotating cylinder is investigated for two types of mentioned cylinders.

Comparison between Figs. 4 and 7 can present the effect of an inner pressure on the response of an FGP cylinder. It indicates that an inner pressure diminishes the maximum value of the radial stress. The decrease is the most for a static cylinder. The radial stress decreases with the increase in the angular velocity.

The same behavior presented above can be expressed for the electrical potential distribution of an FGP rotating cylinder. Comparison between Figs. 2 and 5 indicates that an inner pressure diminishes the maximum value of the radial stress. The decrease is the most for the static cylinder. The electrical potential decreases with the increase in the angular velocity.

5 Conclusions

Comprehensive investigations of the effect of the angular velocity on the mechanical and electrical responses of a rotating FGP cylinder are performed in the present paper. Some related conclusions can be expresses as follows:

(i) The proposed term, named as the additional energy, is defined in the general form, and can be considered in each coordinate system such as the Cartesian system, the cylindrical system, and the spherical system.

(ii) The maximum value of the electrical potential is proportional to the dimensionless angular velocity. This proportionality is not valid for other parameters such as the radial displacement and the radial and circumferential stresses. This relation can be considered in measurement devices for evaluating the angular velocity of the rotating component. Furthermore, the relation can be used in micro-positioning as an actuator. The maximum electrical potential locates near the outer radius. Therefore, two electrodes must be located at the positions of the maximum potential and the inner or outer radius.

(iii) An inner pressure diminishes the maximum value of the radial stress. This decreasing is valid for four angular velocities. Furthermore, the values of the radial stress at a point near the outer radius are identical for five inhomogenous indexes.

(iv) An inner pressure decreases the maximum value of the electrical potential. The applied pressure can also increase the absolute minimum value of the electrical potential.

References

[1] Liu, X., Wang, Q., and Quek, S. T. Analytical solution for free vibration of piezoelectric coupled moderately thick circular plates. *International Journal of Solids and Structures*, **39**, 2129–2151 (2002)

[2] Hou, P. F. and Leung, A. Y. T. The transient responses of magneto-electro-elastic hollow cylinders. *Smart Materials and Structures*, **13**(4), 762–776 (2004)

[3] Kollias, A. T. and Avaritsiotis, J. N. A study on the performance of bending mode piezoelectric accelerometers. *Sensors and Actuators A*: *Physical*, **121**, 434–442 (2005)

[4] Dai, H. L. and Wang, X. Stress wave propagation in piezoelectric fiber reinforced laminated composites subjected to thermal shock. *Composite Structures*, **74**, 51–62 (2006)

[5] Pietrzakowski, M. Piezoelectric control of composite plate vibration: effect of electric potential distribution. *Computers and Structures*, **86**, 948–954 (2008)

[6] Babaei, M. H. and Chen, Z. T. Exact solutions for radially polarized and magnetized magneto-electroelastic rotating cylinders. *Smart Materials and Structures*, **17**(2), 025035 (2008)

[7] Khoshgoftar, M. J., Ghorbanpour, A. A., and Arefi, M. Thermoelastic analysis of a thick walled cylinder made of functionally graded piezoelectric material. *Smart Materials and Structures*, **18**(11), 115007 (2009)

[8] Jabbari, M., Sohrabpour, S., and Eslami, M. R. Mechanical and thermal stresses in a functionally graded hollow cylinder due to radially symmetric loads. *International Journal of Pressure Vessels and Piping*, **79**, 493–497 (2002)

[9] Frank, P. I. *Introduction to Heat Transfer*, John Wiley and Sons, New Jersey, 79–86 (1996)

[10] Kang, J. H. Field equations, equations of motion, and energy functionals for thick shells of revolution with arbitrary curvature and variable thickness from a three-dimensional theory. *Acta Mechanica*, **188**, 21–37 (2007)

[11] Lai, M., Rubin, D., and Krempl, E. *Introduction to Continuum Mechanics*, 3rd ed., Buttenvorth-Heinemann Press, Oxford, 95–108 (1999)

[12] Boresi, A. P., Schmidt, R. J., and Sidebottom, O. M. *Advanced Mechanics of Materials*, 5th ed., John Wiley and Sons, New Jersey, 55–67 (1993)